Morphologies of Dusty Circumstellar Environments

Peter Tuthill, John Monnier & William Danchi

Space Sciences Laboratory, University of California Berkeley, Berkeley, California, 94720-7450, U.S.A.

Chris Haniff

MRAO, University of Cambridge, Cavendish Laboratory, Madingley Rd., Cambridge CB3 OHE, U.K.

Abstract.
We present preliminary results from a program of near-IR diffraction-limited imaging of late-type stars underway at the Keck Observatory. Utilizing the techniques of aperture masking, we transformed the 10 m Keck primary mirror into a separate-element, multiple aperture interferometer. Evolved stars make particularly attractive targets for such a program as they exhibit bright extended emission in the IR which results from astrophysically interesting and poorly understood phenomena such as mass-loss and atmospheric extension. By imaging the hottest regions of circumstellar dust shells at unprecedented angular resolution, we have been able to observe the stellar morphology revealing anisotropic mass-loss in the inner regions where dust nucleation occurs. Furthermore, observations with the Keck telescope have yielded near-IR diameters and images of the stellar photospheres of nearby red giant and supergiants.

1. Introduction

For astronomical sources, such as evolved giants and supergiants, numerous theoretical and experimental studies have underscored the dramatic gains in signal-to-noise ratio (SNR) to be obtained from the use of sparse apertures over more conventional full-pupil speckle interferometry (Roddier 1988, Haniff & Buscher 1992). By masking the pupil of the Keck telescope, we have verified these expected gains in SNR, enabling us to reconstruct complex images with the highest angular resolution in the near-infrared (IR) achieved to date.

With multi-wavelength images spanning the infrared J, H, K and L bands for a number of the brightest Mira variables and evolved supergiants, we have been able to address some of the most pressing questions in the field of late stellar evolution. Amongst the most important of these is mass loss. Although theoretical models usually assume spherical symmetry, there has been a growing body of evidence (e.g. from molecular and polarization data, spectrophotometry, and observations of planetary nebulae) that mass loss can be anisotropic.

Studies in the near-IR are particularly profitable due to the low dust opacity, low contamination from molecular lines, and high luminosity (output peaks in the near-IR). Our measurements of stellar diameters and surface morphologies thus yield information on stellar properties such as pulsational modes, atmospheric structure, giant convective cells and overall photospheric symmetry.

2. Experiment and Observations

Masking of the telescope pupil was achieved by mounting custom-made plates in front of the secondary mirror. The masks were designed with the aid of the CODE V optical ray-trace package. An example showing the hole-pattern of our 15-hole mask, as projected onto the Keck primary mirror, is given in Figure 1. There are many constraints in arriving at such pupil geometries, with the primary concern being to sample the Fourier plane evenly and densely out to the cut-off of the telescope with a *non-redundant* array. Our designs follow from those of Golay (1970), who searched 3-fold symmetric parameter spaces for optimally compact arrays satisfying the condition for non-redundancy; i.e. that no vector baseline occurs more than once. In our case, this search process was greatly complicated by the need to fit the array into the Keck telescope pupil while avoiding sampling across the cracks between segments and blockage by the spiders and undersized secondary.

In order to impart the maximum flexibility in terms of Fourier coverage and object brightness, our program relies on a range of different pupil geometries. In addition to the non-redundant arrays described above, observations were made with annulus-shaped pupils also depicted in Figure 1 (see Haniff & Buscher 1992), and with the fully-filled aperture (FFA). Observations with such pupils confirmed our expectations that far higher levels of photon and atmospheric noise were present compared with non-redundant data. However for faint targets, the extra collecting area more than compensated the gain in noise. Thus the non-redundant arrays were used to obtain the highest SNR data on bright stars, while partially-redundant or FFA geometries could be tailored to optimize observation of dimmer stars.

Light passing through the mask was bought to focus in the Near Infra-Red Camera (NIRC), a cryogenically cooled 256×256 pixel InSb array (Matthews & Soifer 1994). The optical configuration yielded an image scale of 20.57 milliarcsec/pixel – sufficient to Nyquist sample fringes on the longest baselines in K-band.

In common with most high-resolution interferometry and speckle astronomy experiments, it was necessary to use the shortest possible integration times in order to "freeze" the motions within the interference pattern generated by atmospheric turbulence. Ideally the integration time should be less than the atmospheric coherence time ($\sim$50 msec at 2.2 μm), however chip readout limitations dictated an integration time of 134 msec. Although this was not optimal, we were able to recover information on the finest spatial scales from such speckle frames.

An example of a single raw exposure is given in Figure 2. The pattern depicted results from the Airy disks of the small circular sub-apertures being crossed by numerous (105 in this case) fringe patterns arising from interference between each pair of holes. Contributions from each baseline can be separated and measured by taking the power spectrum, as shown to the right, where we

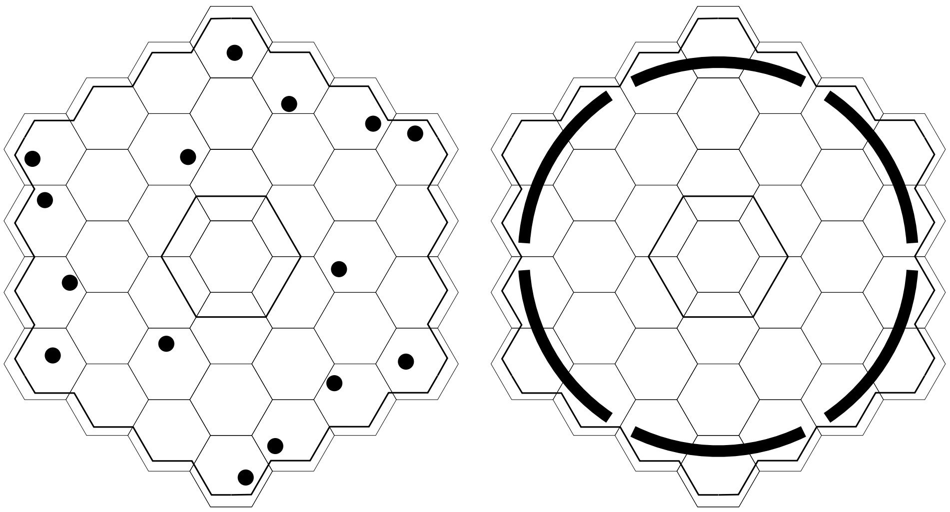

Figure 1. Examples of pupil geometries used for our Keck masking experiment. A 15-hole non-redundant array (left) and an annulus mask (right) are shown superimposed over scaled images of the Keck primary mirror.

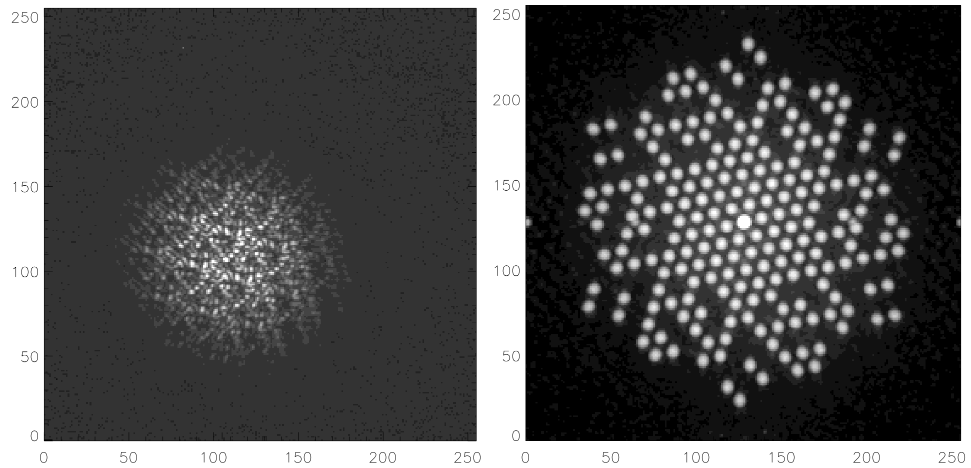

Figure 2. Interferogram of a point-source star taken at $2.2\,\mu$m (left). The 15-hole non-redundant mask depicted in Figure 1 generated this interference pattern. The power spectrum (right panel) is the result of accumulating the power spectra of 100 such raw data frames.

have accumulated the mean spectrum over 100 separate interferograms. It is interesting to note that this illustrates the Fourier coverage afforded by the array, and in this case it can be seen that our sampling out to the limit of the 10 m pupil is extremely good.

Data reduction proceeded by extracting the visibilities and phases from each exposure. Such data are related to the brightness distribution of the science target by a Fourier transform (e.g. Born & Wolf 1964). Although the Fourier phases were corrupted by atmospheric phase fluctuations, an observable known as the *closure phase* – the sum of baseline phases around closed triangles – has been developed in radio astronomy to overcome this problem. These techniques are well established at optical wavelengths (Haniff et al. 1987, Roddier 1988).

Raw visibilities were calibrated for the mean telescope–atmosphere transfer function by utilizing nearly contemporaneous observations of point-source stars. The observing regimen devoted an equal amount of time to such calibration stars, interleaved with the science targets under nearly-identical conditions. Even so, seeing and other changes make the calibration process notoriously difficult and mismatches between source and calibrator data introduced the greatest uncertainty into the final results.

Having obtained a set of calibrated visibilities and closure phases, there are a number of highly developed algorithms to reconstruct images in such a way as to minimize spurious artifacts such as sidelobes arising from the non-uniform and noisy sampling of the Fourier plane. One of the most popular of these, known as the "Maximum Entropy Method" (Gull & Skilling 1984, Sivia 1987), has been used. In order to check the reliability of the reconstructions, the results of MEM have been compared with those from the CLEAN reconstruction algorithm (Högbom 1974), also used widely in radio astronomy. Quantitative information can also be extracted by fitting models directly to the Fourier data.

3. Results

One facet of our science program has focussed on long-period variables. For these stars, an outstanding problem has been the precise determination of their angular diameters (Wood 1990). This has important repercussions for stellar dynamical modeling: precise diameter measurements coupled with good distance estimates provide the most direct method of determining the mode of stellar pulsation. Interferometric observations at optical wavelengths are problematic because the stellar spectrum is blanketed by molecular lines formed in intermediate layers above the continuum photosphere (Scholz & Takeda 1987). Furthermore, measurements in the mid-IR are contaminated by emission from circumstellar dust. Thus the near-IR offers the best hope for measuring the stellar photosphere.

Our diffraction-limited observations with the Keck telescope have enabled us to measure photospheric stellar diameters in a number of near-IR wavebands, as is illustrated in Figure 3. Such high-quality visibility data allows us to address a number of important topics in the study of evolved stars:

1. When combined with distance estimates for a sample of stars (e.g. from Hipparcos), dynamical studies, such as those of Haniff et al. (1995), can

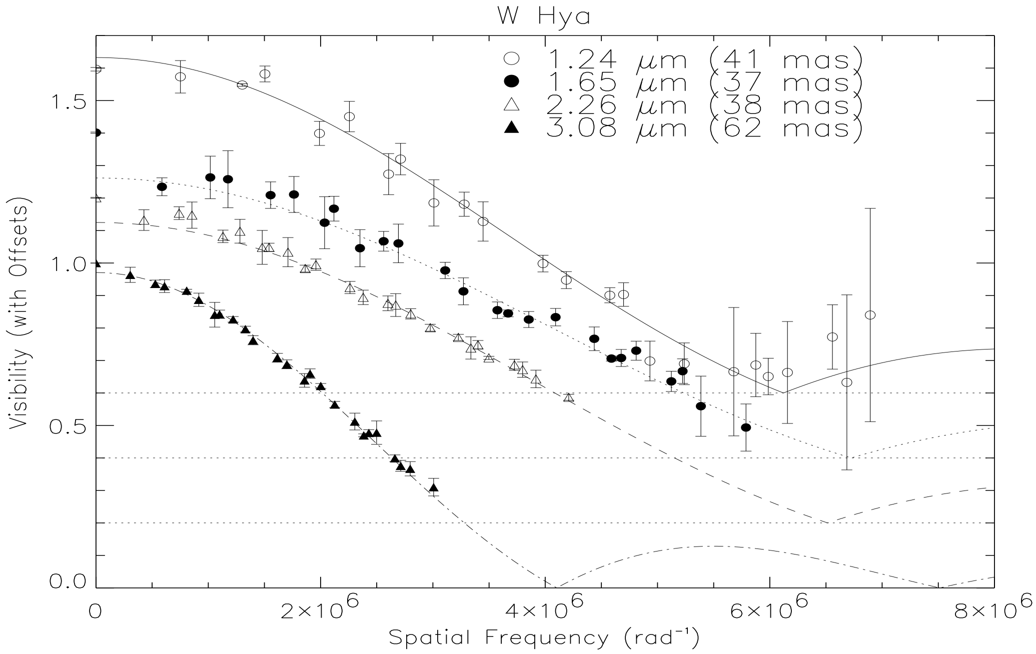

Figure 3. Azimuthally averaged visibility curves produced for W Hya from multi-wavelength speckle data. Diameters given correspond to the best-fit uniform-disk models, which can be seen to be well matched to the data. The larger apparent diameter recorded at $3.08\,\mu$m may be due to molecular or dust blanketing around the star.

determine the pulsation mode and other fundamental dynamical properties.

2. Quasi-monochromatic diameters at a range of wavelengths probe the atmospheric structure, helping to discriminate emission from the photosphere, molecular atmosphere and circumstellar dust, thereby providing valuable experimental testing of numerical model atmospheres.

3. Time-series measurements of stellar diameters through the pulsation cycle should be able to directly observe changes in photospheric radius.

4. Bright asymmetric features, or hotspots, have been detected on the surfaces of late-type stars (Buscher et al. 1990, Tuthill et al. 1997, Gilliland & Dupree 1997), while other workers have reported elliptical distortions of the photosphere (Karovska et al. 1991, Quirrenbach et al. 1992). Our measurements provide images at the highest resolution yet in the near-IR, and can thus help to settle such questions of morphology.

Some of our target sources possess dusty circumstellar halos. At the diffraction limit of the Keck telescope, we were able to resolve these shells for some of the most well-studied, prototypical evolved stars. Spectacular images showing shells, clumps and outflows have been obtained for science targets IRC +10216,

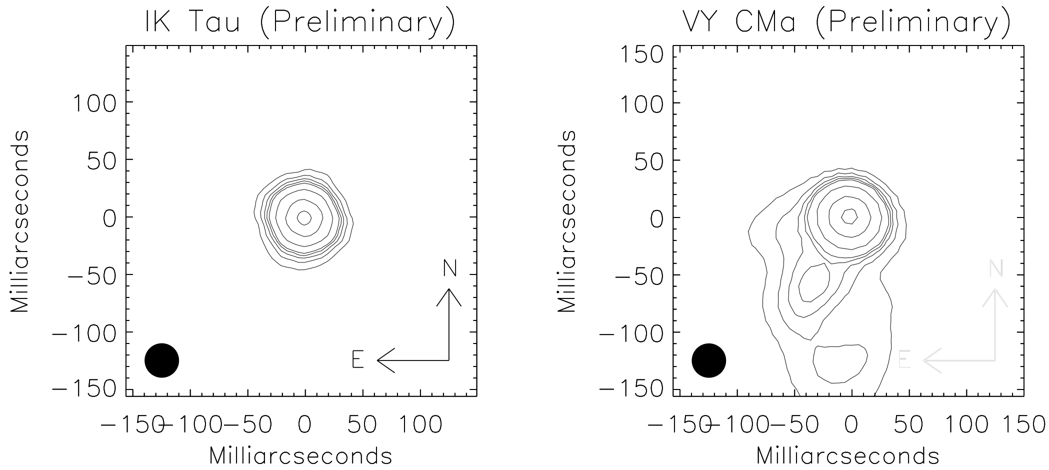

Figure 4. Maps of the Mira variable IK Tau (left) and the supergiant VY CMa (right) at 2.2 μm reconstructed from aperture synthesis imaging data. Contours are 2,4,6,8,10,20,50 and 90 % of the peak.

CIT 6, NML Cyg and VY CMa. To give a flavor of this work within the constraints of this report, we focus here on the enshrouded Mira IK Tau, and the red supergiant VY CMa.

Shell-like structures out beyond the 0.05-0.11$''$ dust condensation radius have been reported for IK Tau from studies mid-IR interferometry (Hale et al. 1997). Our recent Keck image, shown in Figure 4, confirms the presence of significant circumstellar dust, and gives experimental support to the assumption that the outflow is spherically symmetric.

Although optical nebulosity around VY CMa has been known for most of this century, it was not until the imaging polarimetry of Herbig (1972) that bright knots within this structure were revealed as scattering enhancements rather than companion stars as previously thought. More recently, HST/FOC imaging (Kastner 1997) of the visible halo has revealed not only the well-known $\sim$3$''$ extension to the west, but also a complex and dynamic inner region.

The dust formation zone close to the star is best viewed at infrared wavelengths due to the high scattering-induced optical depths in the visible. We present, in Figure 4, images of VY CMa's bright inner the dust envelope at 2.2 μm. Such unprecedented resolution has revealed asymmetric, one-sided thermal emission to the south with a slight spiral structure. This emission is almost certainly a tracer for a dust clump or outflow whose proximity to the photosphere makes it hot enough to radiate in the near-IR.

There is evidence for asymmetries in the mass-loss process coming from polarization studies (Trammel et al. 1994), molecular data, the fitting of spherically-symmetric broad-band spectro-photometric models (e.g. Planesas et al. 1990) and VLBI mapping of maser emission (e.g. Greenhill et al. 1995). However, it has not been possible to image the circumstellar dust of many of these stars at sufficiently high resolution to infer the details of these asymmetries. Our program with the Keck has demonstrated the ability to resolve the hot dust emission on small scales, revealing unambiguous signatures of anisotropic mass-loss close to the stellar surface. This raises intriguing questions as to why mass loss seems to be a fairly spherically symmetrical process in some stars yet not in others. Could this be related to binarity, stellar rotation, or perhaps some other stellar property?

Acknowledgments. We would like to thank Devinder Sivia for the maximum-entropy mapping program "VLBMEM" which we have used to reconstruct diffraction-limited images. This work has been supported by grants from the National Science Foundation and the Office of Naval Research.

References

Born M. & Wolf E. 1964, *Principles of Optics*, Macmillan, New York.

Buscher D.F., Baldwin J.E., Warner P.J. & Haniff C.A. 1990 MNRAS, **245**, 7B

Gilliland R.L. & Dupree A.K. 1997, ApJ, **463**, L29

Golay M. 1971, *J. Opt. Soc. Am.*, **61**, 272

Greenhill L.J., Colomer F., Moran J.M., Backer D.C., Danchi W.C., & Bester M. 1995, ApJ, **449**, 365.

Gull S.F. & Skilling J. 1984, *IEEE Proceedings*, **131**, Pt. F, No. 6

Hale D., Bester M., Danchi W.C., Hoss S., Johnson M., Lipman E.A., Lopez B., Monnier J.D., Tuthill P.G., Geballe T.R., and Townes C.H. 1997 ApJ, In Press.

Haniff C.A., Mackay C.D., Titterington D.J., Sivia D., Baldwin J.E. & Warner P.J. 1987, *Nature*, **328**, 694

Haniff C.A. & Buscher D.F. 1992, *J. Opt. Soc. Am.*, *A*, **9**, 203

Haniff C.A., Scholz M. & Tuthill P.G. 1995, MNRAS, **266**, 745

Herbig G.H. 1972, ApJ, **172**, 375

Högbom J. 1974 ApJS, **15**, 417

Karovska M., Nisenson P., Papaliolios C., Boyle R.P. 1991, ApJ, **374**, L51

Kastner J.H., 1997 *Hubble Archive*, proposal GO-6416

Matthews K, & Soifer B.T. 1994, Ap&SS*190* 239

Planesas P., Kenney J., Bachiller R. 1990, ApJ, 364, L9

Quirrenbach A., Mozurkewich D., Armstrong J.T., Johnston K.J., Colavita M.M. & Shao M. 1992, A&A, **259** L19

Roddier F. 1988, *Physics Reports*, **170**, 97

Scholz M. & Takeda Y. 1987, A&A, **186**, 200

Sivia D.S. 1987, *Ph.D. Dissertation*, Cambridge University

Trammel S.R., Dinerstein H.L. and Goodrich R.W. 1994, AJ, 108, 984

Tuthill P.G., Haniff C.A. & Baldwin J.E. 1997, MNRAS, **285** 529

Wood P.R. 1990, in Mennessier M.O. & Omont A., (eds) Editions Frontières, Gif-sur-Yvette, P.67